

Repeat Sequence of Epstein-Barr Virus-encoded Nuclear Antigen 1 Protein Interrupts Proteasome Substrate Processing*

Received for publication, September 22, 2003, and in revised form, December 3, 2003
Published, JBC Papers in Press, December 19, 2003, DOI 10.1074/jbc.M310449200

Mingsheng Zhang and Philip Coffino‡

From the Department of Microbiology and Immunology, University of California, San Francisco, California 94143

The Epstein-Barr virus thwarts immune surveillance through a Gly-Ala repeat (GAR) within the viral Epstein-Barr virus-encoded nuclear antigen 1 protein. The GAR inhibits proteasome processing, an early step in antigen peptide presentation, but the mechanism of proteasome inhibition has been unclear. By embedding a GAR within ornithine decarboxylase, a natural proteasome substrate that does not require ubiquitin conjugation, we now demonstrate inhibition in a purified system, excluding involvement of ubiquitin conjugation or of proteins extraneous to substrate and proteasome. We show further that the GAR acts as a stop-transfer signal in proteasome substrate processing, resulting *in vivo* in partial proteolysis that halts just short of the GAR. Similarly, introducing a GAR into green fluorescent protein destabilized by the ornithine decarboxylase degradation domain also stops the progress of proteolysis, leading to the accumulation of partial degradation products. We postulate that the ATP motor of the proteasome slips when it encounters the GAR, impeding further insertion and, in this way, halting degradation.

Viruses use diverse strategies to subvert host defense mechanisms. The immune response offers a prominent target for such attacks (1, 2). Mounting a host immune response requires cleaving viral proteins to peptides and then presenting these as antigenic epitopes. The Epstein-Barr virus (EBV)¹-encoded nuclear antigen 1 (EBNA1) protein of EBV is the sole viral protein required for genome replication in latent infections and is uniformly expressed in malignant cells that arise from EBV infection (3). Within the EBNA1 protein lies a long repetitive sequence composed exclusively of glycine and alanine residues. Among different viral isolates, the repeat sequence ranges in size from about 60 to 300 residues (4). This sequence thwarts immune surveillance by forestalling presentation of EBNA1-derived peptides (5). Antigenic peptides cannot be generated from the intact protein but can be produced from forms of EBNA1 which lack the repetitive sequence. The Gly-Ala repeat (GAR) restricts the immune response by preventing cleavage of EBNA1 by the proteasome (6); recent evidence shows that the

GAR also inhibits EBNA1 translation (7). Proteasomes are the major neutral protease of eukaryotic cells and the major source of antigenic peptides presented by major histocompatibility complex class I molecules. The proteasome consists of two large protein complexes (8). Its 20S catalytic core contains proteolytic sites concealed within a hollow cylindrical nanochamber. Access to the chamber lies through ports in the cylinder ends. A 19S regulatory complex is present at one or both ends of the cylinder. It comprises six distinct ATPases, all essential, and about a dozen additional proteins. Functions attributed to the 19S complex include substrate recognition, unfolding, and insertion into the catalytic cylinder.

Fusion of GAR to diverse proteasome substrates has been found to reduce their turnover by the proteasome (9–11). GAR can thus function as a context-independent *cis*-inhibitory module. In most cases, processing by the proteasome requires that substrates first be modified by conjugation to multiple copies of the 76 amino acid ubiquitin protein (12). Although a GAR sequence does not prevent this modification (6), it is difficult to exclude quantitative or qualitative changes in ubiquitin conjugation. Some downstream step in the ubiquitin-proteasome degradation pathway is likely altered, but the nature of the impairment is not clear. Furthermore, providing EBNA1 with highly potent signals for ubiquitination can override the effect of a GAR, resulting in degradation by the proteasome and antigen presentation (13). Through a mechanism that remains undetermined, GAR potency, a function of repeat sequence length, thus seems to be poised against the extent or efficacy of ubiquitin conjugation.

To examine the mechanism of GAR action, we utilized a natural substrate of the proteasome that does not require ubiquitin modification for degradation (14, 15). Ornithine decarboxylase (ODC) has a short half-life that is modulated by interaction with the protein antizyme 1 (AZ1) (16). ODC initiates the biosynthesis of polyamines. Excess polyamines accelerate the production of AZ1, which interacts with ODC to enhance the affinity of ODC for proteasomes (15). The trio of ODC, AZ1, and proteasome thereby comprise a feedback mechanism which enables polyamine pools to keep biosynthesis in check by controlling ODC turnover. The well understood structural and functional requirements for ODC degradation provide a test bed for investigating the GAR. In particular, because degradation of ODC is proteasome-mediated but independent of ubiquitin conjugation, it offers a context for investigating whether GAR action is limited to ubiquitin-conjugated proteasome substrates. We show here that a 30-residue GAR embedded in ODC strongly inhibits degradation of ODC by the proteasome. However, biochemical competition experiments showed that the repeat sequence does not impair proteasome-ODC interaction. The GAR must, therefore, function at a step downstream of substrate recognition by the proteasome. This conclusion was substantiated by the observation that *in vivo* degradation ini-

* The work was supported by National Institutes of Health Grant R01 GM-45335. The costs of publication of this article were defrayed in part by the payment of page charges. This article must therefore be hereby marked "advertisement" in accordance with 18 U.S.C. Section 1734 solely to indicate this fact.

‡ To whom correspondence should be addressed: 513 Parnassus Ave., Dept. of Microbiology and Immunology, UCSF, San Francisco, CA 94143-0414. Tel.: 415-476-1783; Fax: 415-476-8201; E-mail: pcoffin@itsa.ucsf.edu.

¹ The abbreviations used are: EBV, Epstein-Barr virus; EBNA1, EBV-encoded nuclear antigen 1; GAR, glycine-alanine repeat sequence; ODC, ornithine decarboxylase; AZ1, antizyme 1; cODC, carboxyl-terminal degradation domain of ODC; GFP, green fluorescent protein; HA, hemagglutinin.

tiates at an undiminished rate, but then halts if the GAR is present. Degradation stops near the junction of the ODC degradation recognition element and the GAR. The repeat sequence can therefore act as a stop-transfer signal.

EXPERIMENTAL PROCEDURES

Reagents—Methionine assay medium was purchased from Difco, protease inhibitor mixture tablets from Roche, MG132, cycloheximide, anti-FLAG M2 affinity gel from Sigma, anti-His₆ antibody and anti-HA antibody from Santa Cruz Biotechnology, and anti-GFP antibody from BD Biosciences. Sheep anti-mouse IgG horseradish peroxidase conjugates, goat anti-rabbit IgG horseradish peroxidase conjugates, and protein A agarose were all from Amersham Biosciences.

Plasmid Construction and Protein Purification—All plasmid constructions utilized standard molecular biology techniques (17). Constructions that utilized PCR steps were verified by sequencing; constructions that relied on restriction-ligation utilized fully sequenced constituents. *Escherichia coli* expression vectors for mouse ODC and carboxyl 37 amino acid truncated ODC were generated from vector pQE30 (Qiagen) as described (15). Mouse ODC with a GAR positioned after residue 424 was constructed as follows. First, a short sequence with flanking MluI/NdeI sites was cloned after the codon for residue 424 of ODC. After deleting a redundant NdeI site from the pQE30 vector, the ODC open reading frame with insert at 424 was cloned into the remaining NdeI site of the modified vector. For assembly of Gly-Ala 30 repeat with flanking N-terminal FLAG tag and C-terminal HA tag, 4 oligonucleotides were synthesized: GA1, CGCGTACTACAAAGACG-ATGACGACAAGGCTGGAGCAGGCGGTGGAGCAGGTGCTGGAGG-TGCAGGTGGAG; GA2, CCTGCTCCACCTGCACCTCCAGCACCTGC-TCCACCGCCTGCTCCAGCCTTGTGCTCATCGTCTTTGTAGTCA; GA3, CAGGCGGTGCAGGAGCAGGTGCTGCAGGTGCTGGAGGTGG-AGCAGGTTACCCATACGACGCTCCAGACTACGCTCA; and GA4, TATGAGCGTAGTCTGGAGCGTGTATGGGTAACTGCTCCACCTC-CAGCACCTGCACACCTGCTCCTGCACCG.

GA1/GA2 and GA3/GA4 were annealed and phosphorylated by T4 kinase, digested by MluI/NdeI, and ligated to the similarly digested vector carrying ODC with MluI/NdeI sites at position 424. Expression in *E. coli* and purification of recombinant proteins was as described (15). The synthetic protein module created in this fashion encodes (using single letter amino acid code) GSTR (linker1), DYKDDDDK (FLAG epitope), AGAGGGAGAGGAGGAGGAGGAGGAGGAG (Gly-Ala repeat), YPYDVPDYA (HA tag), and HMID (linker2). The 30-residue GA repeat is identical to the amino acid sequence of human EBNA-1 protein, strain B95-8, GI:59074, residues 196–225 (18, 19). The open reading frame consisting of ODC with this module inserted after position 424 is referred to as ODC::GAR. A construct otherwise identical, but with a shorter seven-residue GAR (AAGGGAG) was constructed by similar means and is referred to as ODC::GAR7. Constructs for expression of GFP and GFP destabilized by the addition of the C-terminal 37 amino acids of ODC were made as described (20). The GAR module was inserted as described above.

For use as SDS-PAGE molecular mass markers, recombinant proteins derived from ODC were made in *E. coli* and purified by Talon His₆ affinity chromatography (Clontech). The structure and calculated molecular masses of these proteins were MRGS(H)₆GSACEL-ODC residues 2–461::GAR, 57.7 kDa; MRGS(H)₆-tobacco etch virus protease cleavage site (seven residues)-GSM-(FLAG epitope)-ODC residues 2–461, 54.6 kDa; MRGS(H)₆-(FLAG epitope)-ODC residues 2–445, 51.6 kDa.

For yeast expression, ODC coding sequences were subcloned (SpeI/XhoI digestion) into the p414ADH vector with TRP selection marker (21). A C441A mutant of ODC was generated with a QuikChange site-directed mutagenesis kit (Stratagene). Vectors were transformed into yeast strain MHY501 (*MATα his3-Δ200 leu2-3,112 lys2-801 trp1-1 ura3-52*) (22).

Purification of 26S proteasomes from rat liver, radiolabeling of proteins in *E. coli* and *in vitro* proteasome degradation and competition assays were done exactly as described (15). *In vitro* degradation was assessed by examining the rate of labeled substrate degradation using 7.5 and 10% acrylamide SDS-PAGE (Fig. 1) or by measuring the rate of production of acid soluble counts from labeled substrate (Fig. 2). SDS-PAGE autoradiogram band intensity was quantitated by scanning and analyzing with TotalLab version 2.00 software (Phoretix) in fully automatic mode using rolling circle background subtraction.

Metabolic Labeling, Immunoprecipitation, and Immunoblotting in Yeast—Pulse-chase analysis was carried out exactly as described (20), except that 7.5% Ready-Gel (Bio-Rad) was used for SDS-PAGE. Meta-

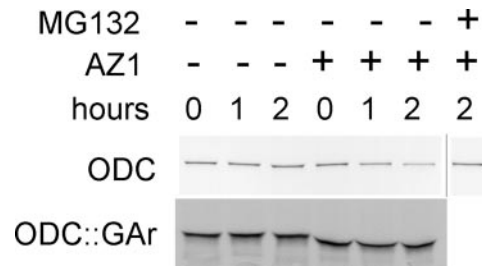


FIG. 1. ODC and ODC::GAR degradation by purified 26S proteasomes. The extent of recombinant protein degradation was determined in the course of 2-h reactions containing purified proteasomes and in the presence or absence of AZ1, as indicated. The effect of the proteasome inhibitor MG132 on ODC degradation was tested.

bolic pulse-chase labeling experiments using the proteasome inhibitor MG132 (23) were performed in an *rpn4Δ* deletion strain of genotype *MATα his3-Δ200 leu2-3, 112 lys2-801 trp1-1 ura3-52 rpn4Δ::kan MX4* (20). An overnight culture was diluted to $A_{600} = 0.15$ with medium containing 50 μ M MG132 (or Me₂SO solvent for untreated controls) and incubated for 6 h before pulse label and chase, and performed as described above, except that 50 μ M of MG132 was also included in the pulse and chase buffers. For cycloheximide chase, 20 ml of yeast transformant cultures in exponential growth phase ($A_{600} 0.2$ – 1.0) were harvested by centrifugation (3 min, $2000 \times g$) and washed once with 1 ml of S.D. medium (20). The cells were resuspended in 0.5 ml of chase medium (S.D. medium with 0.5 mg/ml cycloheximide). Incubation was continued at 30 °C, and at each time point, 125 μ l of cells were removed, centrifuged, resuspended in 125 μ l of lysis buffer, and transferred to a 2-ml screw-top microcentrifuge tube containing 200 μ l of 0.5-mm glass beads. Cells were lysed as in the pulse-chase assays. For immunoprecipitation with anti-His₆ antibody, 400 μ l of lysate in lysis buffer was incubated for 1 h at 4° with 2 μ l of anti-His₆ antibody. 20 μ l of protein A agarose was added, and after an additional 1 h of incubation, samples were prepared for Western blotting. Immunoaffinity matrix beads were collected by brief centrifugation ($2000 \times g$ for 20 s) and washed 4 times with 1 ml of lysis buffer containing 0.1% SDS. To recover soluble samples for 7.5% acrylamide SDS-PAGE fractionation, the beads were resuspended in SDS sample buffer (29) and heated to 100° for 5 min. 20 μ g of protein/lane were loaded for Western blotting. Immunoprecipitation with anti-FLAG was identical, except that the antiserum was purchased covalently linked to anti-FLAG M2 affinity gel (Sigma).

RESULTS

GAR Inhibits Proteolysis by Purified Components—The degradation element of mammalian ODC consists of its 37 carboxyl-terminal residues cODC. Grafting cODC to other proteins causes them to associate with the proteasome and converts them to proteasome substrates (15, 20). Depriving ODC of cODC has no effect on its enzymatic specific activity, implying that acquiring a native conformation does not require that the C terminus be present. Crystallographic models are consistent with the conclusion that cODC is a structurally distinct domain (24). For these reasons, the junction of cODC with the remainder of the protein is an obvious place to insert sequences that could alter its turnover properties. We arbitrarily chose from within a longer EBV EBNA1 GAR sequence the 30-residue subsequence AGAGGGAGAGGAGGAGGAGGAGGAGGAGGAGGAG. To facilitate analysis required in experiments reported below, we flanked the GAR sequence with a FLAG epitope (DYKDDDDK) on the N-terminal side and an HA epitope (YPYDVPDYA) on its C-terminal side. This linker1-FLAG-GAR-HA-linker2 module was inserted after residue 424 of the 461 amino acid ODC protein to create ODC::GAR. Recombinant ODC and ODC::GAR had indistinguishable specific enzymatic activity and reactivity with AZ1 (results not shown). As reported previously, highly purified rat proteasomes degraded native ODC (without the GAR), and degradation depended upon the addition of AZ1 (Fig. 1, top). In sharp contrast, ODC::GAR was not measurably degraded in this assay (Fig. 1, bottom). Evaluating the release of soluble counts from a labeled sub-

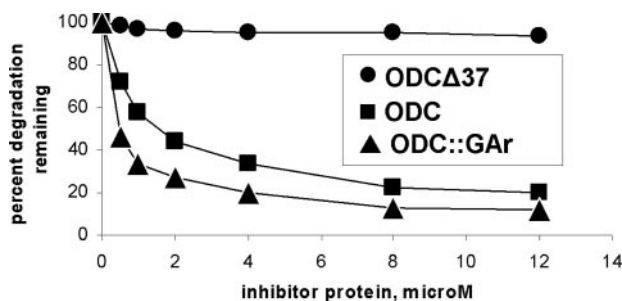


FIG. 2. **Competitive inhibition of ODC degradation by ODC, ODC Δ 37, and ODC::GAR.** Data is normalized to ODC degradation observed in the absence of competing inhibitor protein and is expressed as percent residual degradation. Incubations were for 30 min and contained 100 nM proteasome, 50 nM radiolabeled ODC, and various concentrations of inhibitor proteins, as indicated.

strate protein rather than disappearance of substrate, as in Fig. 1, offers a more sensitive way to determine the extent of degradation. For ODC, 15.6% of input counts were made soluble in the presence of AZ1 in 40 min *versus* 3.0% without AZ1; for ODC::GAR, these figures were 1.7 and 2.2%, respectively. Insertion of a GAR sequence evidently strongly inhibits ODC degradation, as reported for other proteins in cells and in crude extracts containing proteasomes (25). It can also do so, as shown here, in a reaction containing only purified components.

Neither Proteasome Interaction nor Catalytic Function Are Impaired by the GAR—One possible explanation of this finding is that the GAR prevents interaction between ODC and the proteasome. We used a competition assay (15) to test this idea. Radiolabeled ODC was incubated with limiting amounts of proteasomes together with various amounts of unlabeled competing proteins, and the extent of ODC degradation was determined by measuring the time-dependent release of soluble radiolabel. The competitors were ODC (structurally identical to the labeled substrate), a truncated form of ODC (ODC Δ 37, which lacks the C-terminal ODC degradation element), and ODC::GAR (Fig. 2). As described previously, ODC acts as a competitive inhibitor ($IC_{50} \sim 2 \mu M$) (15). Although both ODC::GAR and ODC Δ 37 failed to undergo degradation (Fig. 1), ODC::GAR is at least as potent as ODC in the competition assay ($IC_{50} \sim 0.5 \mu M$), in sharp contrast with ODC Δ 37, which is inactive. We conclude that the GAR insert does not render ODC incompetent for interaction with proteasomes and must, therefore, act to prevent degradation at a step subsequent to proteasome recognition. To determine whether ODC::GAR acts to inhibit the catalytic function of the proteasome, we measured the effect of that protein on the peptidase activity of proteasomes, using the identical reaction conditions as in Fig. 2. The various forms of ODC, together with AZ1, were introduced at concentrations as high as 1000-fold the proteasome concentration to maximize our chance of seeing an effect. However, we observed no change in proteasome-mediated peptide hydrolysis upon incubation with ODC, ODC Δ 37, or ODC::GAR (results not shown). The inhibitory effect of the GAR must, therefore, target some step that lies between recognition and catalysis.

GAR Insert Causes Partial Proteolysis—Degradation of ODC has similar structural requirements *in vitro* and *in vivo*, but degradation is more rapid in living cells. Yeast expression was used to determine more sensitively whether ODC containing a GAR could be processed by the proteasome. Mammalian ODC turnover has similar characteristics in animal cells and in yeast: it is mediated by the proteasome and is sensitive to mutation of the same critical residues in the ODC C-terminal region (20). In yeast, mammalian ODC has a half-life of about 10 min (20, 26). Unlike animal cells, in which AZ1 has a very marked effect on ODC turnover, co-expression of AZ1 acceler-

ates ODC turnover only about 2- to 3-fold. Therefore, we can use this *in vivo* model of mammalian ODC degradation without the need to co-express AZ1. Pulse-chase experiments in yeast with ODC::GAR were performed using anti-FLAG antibody for immunoprecipitation, and the results were evaluated by 10% acrylamide SDS-PAGE, as in the *in vitro* degradation experiments. ODC::GAR was seen to undergo time-dependent changes in mobility during the course of the 60 min chase period (results not shown). To better resolve protein species that appeared in the course of the chase, we utilized 7.5% acrylamide SDS-PAGE gels. These fractionation conditions revealed a prominent parent band seen at the end of the 5 min pulse label period, which corresponded to the beginning of the chase period; this band diminished in the course of the chase and was replaced by a trio of bands of greater mobility, the fastest-moving being less intense than the other two (Fig. 3A, top). The proteins that appeared during the chase, the products of ODC::GAR post-translational processing, have been termed band 1 (slowest), band 2, and band 3 (fastest).

Similar pulse-chase analysis of ODC without the GAR module (Fig. 3A, second from top) showed, as reported previously, that the protein turns over with a half-life of ~ 15 min. (In an additional control experiment, ODC::GAR0, containing the GAR module but with no Gly-Ala residues present, was completely degraded and had the same kinetics as ODC (results not shown)). Importantly, both ODC::GAR and ODC disappeared at a similar rate (Fig. 3B), implying that the initial steps of their proteolysis proceed according to identical mechanisms. Pulse-chase analysis under identical conditions, but using a GAR insert of 7 residues rather than 30 (ODC::GAR7, Fig. 3A, third from top), also revealed the production of a partial proteolysis product, with mobility similar to that of band 1. For ODC::GAR (with the 30-residue GAR), the sum of the intensities of precursor and product bands was approximately constant during the entire 60-min chase period, which is consistent with a highly efficient block following partial ODC::GAR degradation. In significant and reproducible contrast, the sum of parent and product band densities diminished during the ODC::GAR7 chase period: in the representative experiment shown, only 42% of the total density present at 0 min was still present at 30 min; 38% was still present at 60 min. This result shows that less than half of the radiolabeled ODC::GAR7 protein pool undergoes partial proteolysis, and the rest is fully degraded. Within the size range examined, GAR length determines the efficiency of blocking further degradation of partial proteolysis products derived from ODC. The greater efficacy of GAR30 compared with GAR7 is consistent with previous findings that a longer GAR is a more effective inhibitor of degradation (11). The rate at which ODC, ODC::GAR7, and ODC::GAR diminished was indistinguishable (Fig. 3B). However, the products of ODC::GAR7 and ODC::GAR (with 30 GAR residues) differed in two ways: (i) the longer GAR produced three bands which together accounted for all the products of the parent band; and (ii) the shorter GAR produced only one partial degradation product (similar in mobility to band 1 of the partial proteolysis trio), and this single band accounted for only a part of the products of parent band proteolysis.

The role of the proteasome in the production of bands 1–3 was tested in two ways. Mutation of residue Cys⁴⁴¹ of native ODC has been shown to prevent ODC proteasome degradation in both animal cells and in yeast (15, 20, 27). Introducing a C441A mutation in ODC::GAR stabilized the protein and prevented the appearance of bands 1–3 during a pulse-chase experiment (Fig. 3A, bottom). This finding, therefore, implies that proteasomes produce the slower-migrating species by partially digesting ODC::GAR. Next, we showed that a proteasome in-

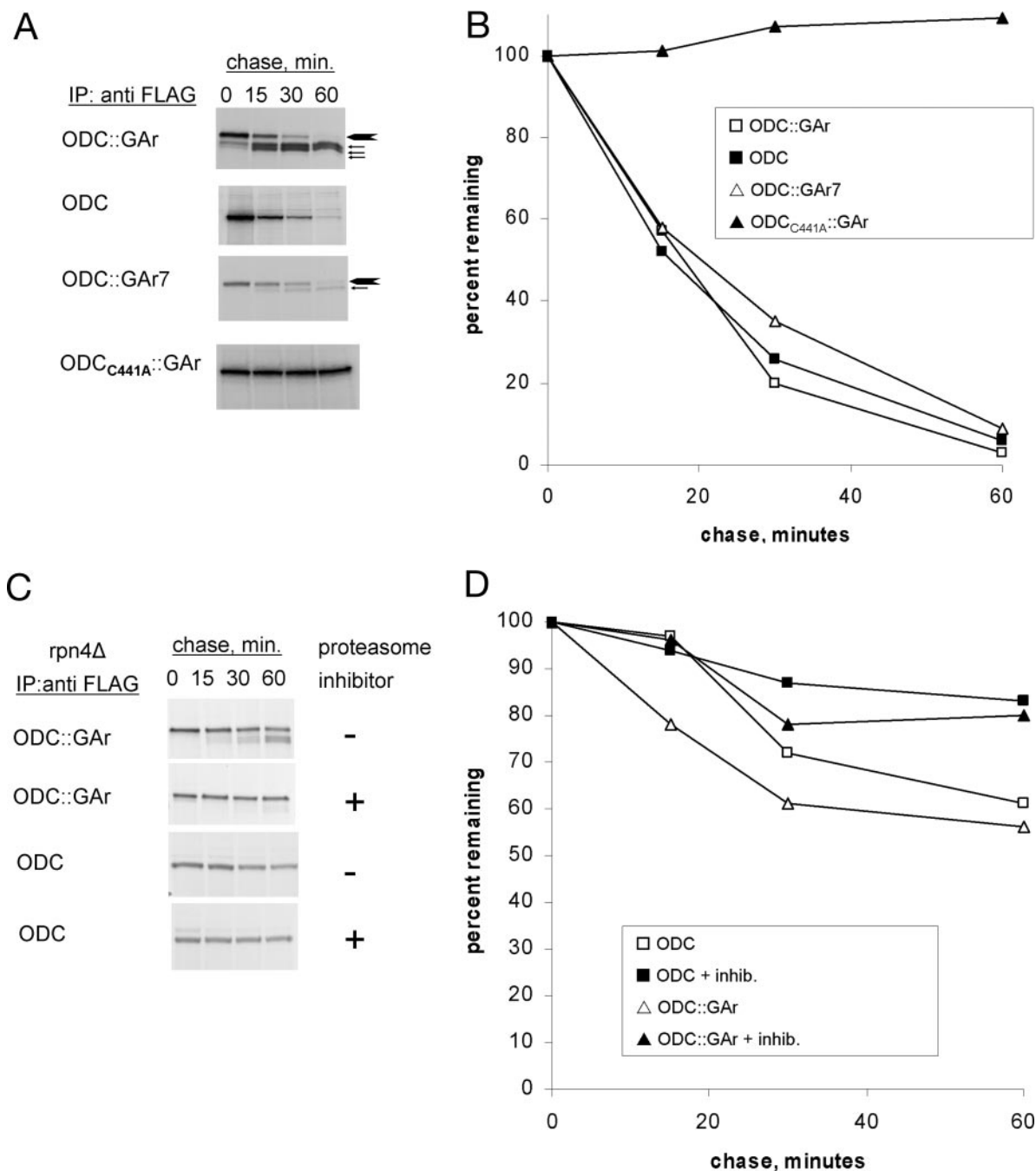


FIG. 3. Pulse-chase analysis of processing. A, cells expressing ODC::GAR (repeat length 30), ODC, ODC::GAR7 (repeat length 7), or ODC_{C441A}::GAR were [³⁵S]methionine-labeled and then chased in unlabelled medium. Samples were removed periodically, and extracts were immunoprecipitated with anti-FLAG affinity gel and fractionated by SDS-7.5% PAGE. Arrowheads, ODC with GAR insertions; arrows, bands corresponding to individual processed proteins. B, quantitation of ODC::GAR, ODC, ODC::GAR7, and ODC_{C441A}::GAR bands shown in A. C, effect of the proteasome inhibitor MG132 on processing. Cells were *rpn4Δ*, a mutation that makes them susceptible to the inhibitor. D, quantitation of ODC and ODC::GAR bands shown in C.

inhibitor prevented the production of bands 1–3. Pharmacologic proteasome inhibitors are relatively ineffective in wild-type yeast (28) but are more effective in strains lacking the Rpn4 protein, a positive transcriptional regulator of proteasome-associated genes. By preventing compensatory changes in proteasome function, mutating Rpn4 makes it possible to use highly specific proteasome inhibitors in yeast (20, 29). In an *rpn4Δ* deletion strain, ODC::GAR turned over with a half-life of more than 60 min (Fig. 3C, top and D). The half-life of both ODC::GAR and ODC is prolonged severalfold in *rpn4Δ* cells compared with Rpn4 wild-type cells (compare Refs. 20, 26, and Fig. 3A), presumably because proteasome-associated genes are

down-regulated. The peptide aldehyde proteasome inhibitor MG132 impaired ODC::GAR degradation and almost completely prevented production of the minor bands (Fig. 3C, second from top, and D), confirming the inference that proteasomes produce the smaller proteins by partially cleaving ODC::GAR. ODC was also stabilized by the inhibitor (Fig. 3C, bottom pair of gels, and D). As was observed in unperturbed cells with wild-type Rpn4 protein (Fig. 3, A and B), ODC and ODC::GAR were degraded in *rpn4Δ* cells at similar rates, albeit at a slower absolute rate than in cells with intact Rpn4 expression (Fig. 3D).

Partial Proteolysis Stops Short of the GAR—To determine the

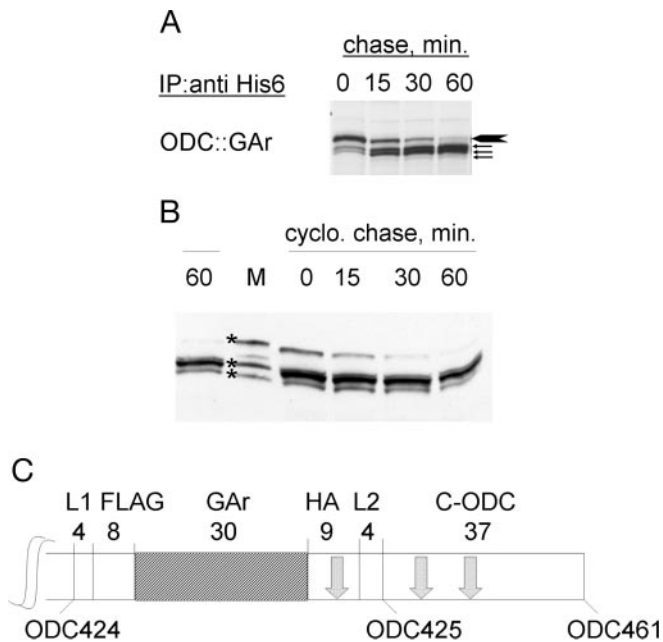


FIG. 4. Carboxyl-terminal truncation and molecular mass of processed proteins. *A*, pulse-chase analysis, as in Fig. 3A, but using the amino-terminal His-6 tag for pull-down. *B*, Western blot analysis with anti-FLAG antibody of protein size standards (*lane M*) versus ODC::GAR and its product proteins. Cells were treated with cycloheximide for the times indicated (60-min sample repeated to *left* of marker lane). The marker proteins (*asterisks*) were a mixture of three FLAG-tagged proteins derived from ODC produced in *E. coli*, with predicted molecular masses of 57.7, 54.6, and 51.6 kDa. ODC::GAR has a predicted molecular mass of 56.8 kDa. Bands 1–3 have mobility corresponding to molecular masses of 54.8, 53.7, and 51.9 kDa, respectively. *C*, schematic of ODC::GAR C-terminal region showing components of GAR module, with GAR sequence *cross-hatched*. The number of amino acids of each component is shown; *arrows* mark the estimated position of truncation of processed proteins.

structural relationship of bands 1–3 to ODC::GAR, cells expressing that protein were subjected to pulse-chase conditions, and labeled extracts were purified as above, but now using the His₆ tag at the N terminus for immuno-purification, rather than the internally positioned FLAG epitope, which lies just to the N-terminal side of the GAR sequence. Labeled proteins recovered using the His₆ tag showed a similar band pattern as those recovered with the FLAG tag (Fig. 4, compare Fig. 3A, *top*). As His₆-containing proteins must retain the N terminus, bands 1–3, if due to partial terminal proteolysis, must arise from truncation at the C terminus. To better determine the extent of truncation of the proteins associated with the minor bands, we generated a set of FLAG-tagged molecular mass standards consisting of variants of ODC (Fig. 4B, *lane M*). Bands 1–3 were produced by treating yeast-expressing ODC::GAR with cycloheximide to inhibit protein synthesis; samples were collected periodically. During the 60 min course of cycloheximide treatment, labile proteins should diminish, but their post-translational products, if stable, should remain little changed in amount. Western blot analysis with anti-FLAG antiserum revealed a time-dependent reduction of ODC::GAR; as expected, its putative stable proteolysis products did not change markedly with time (Fig. 4B). The pattern of product bands was similar to that seen above with pulse-chase analysis, but quantitative differences are apparent: band 3 is now more distinctly seen, and band 1 is fainter, almost merging with band 2. By comparing the mobility of bands 1–3 with that of the ODC-derived molecular size markers, we estimate bands 1–3 to correspond in mobility to proteins lacking ~20, ~30, and ~45 residues, respectively, from the C terminus. Fig. 4C de-

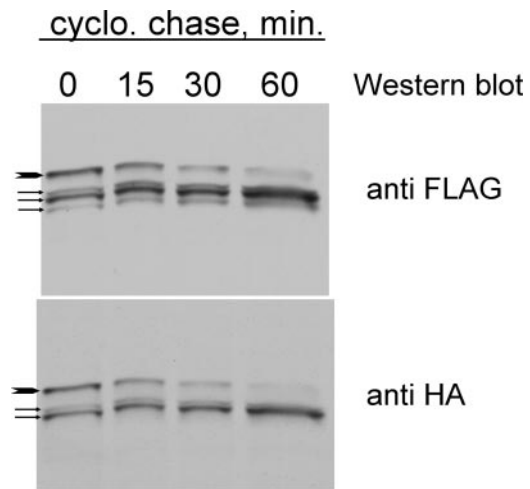


FIG. 5. Comparative Western blot analysis with anti-FLAG and anti-HA antibodies of ODC::GAR and its product proteins. *Arrowhead*, ODC::GAR; *arrows*, processed proteins.

picts a protein structure schematic and the position of the inferred sites of cleavage.

The modular GAR insert present in ODC::GAR serially contains linker1-FLAG-GAR-HA-linker2 (see “Experimental Procedures”). As linker2 is four residues in size and the module is inserted 37 residues from the C-terminal end of ODC, the HA epitope begins 41 residues from the end and should, therefore, be partially destroyed in the fastest-moving species, postulated to lack ~45 C-terminal amino acids. To test this expectation, Western blot analysis of cycloheximide-treated cells expressing ODC::GAR was performed with antisera directed against either the FLAG or HA epitopes (Fig. 5, *top* and *bottom*, respectively). A similar pattern was seen with both antisera, except that the fastest-moving band among the product cluster was visualized with anti-FLAG antiserum but not with anti-HA. This result confirms our hypothesis that the product species arise from truncating ~20, ~30, and (more rarely) ~45 residues from the C terminus of ODC::GAR. The degradation process must, therefore, stop short of the GAR tract, the proximal end of which lies 50 residues from the C terminus.

A GAR Also Leads to Partial Proteolysis of Destabilized GFP—To determine whether GAR-induced partial proteolysis is restricted to ODC, we examined the degradation of a protein containing GFP in place of most of the ODC coding sequence. We have shown previously that appending the terminal 37 amino acids of mouse ODC (cODC) to GFP destabilizes that reporter protein in yeast (20), as it does in animal cells (30). Using yeast cell expression, we compared GFP-cODC to GFP-GAR-cODC; in the latter, the GAR 30-residue module is placed between the GFP and cODC sequences. This pair of constructs is thus identical to those analyzed above, but with GFP replacing residues 1–424 of ODC, that is, most of the protein. We used cycloheximide chase and Western blot analysis (with anti-GFP antibody) to examine the turnover of the expressed proteins and the relationship between parent and product species. As described previously (20), appending cODC destabilized GFP, and GFP-cODC was completely degraded, producing no detectable partial degradation products (Fig. 6). We found that GFP-GAR-cODC generated a trio of bands (Fig. 6), much as was seen with ODC::GAR (Fig. 5, *top*). Mutating the cysteine 441 residue within the ODC C terminus, which is critical for proteasome degradation (15, 20, 27), stabilized the parent GFP-GAR-cODC protein and prevented the appearance of the trio of derived products. As was true for the ODC and ODC::GAR pair, the GFP-cODC and GFP-GAR-cODC parent bands diminished

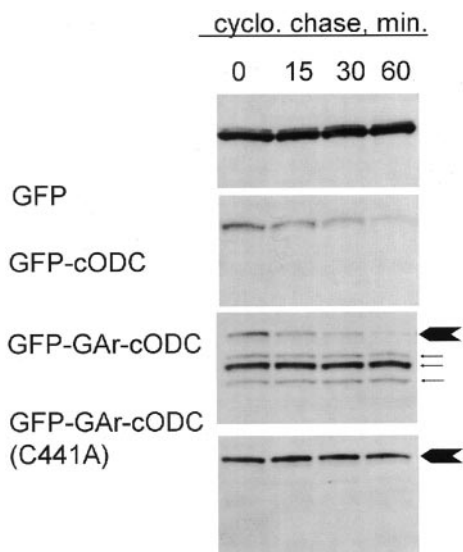


FIG. 6. Cycloheximide chase Western blot analysis of destabilized GFP with GAR. Yeast expressing the indicated forms of GFP were analyzed as in Fig. 5, but with anti-GFP antiserum for immunoblotting.

at a similar rate during the chase. In cultured animal cells, fusing a GAR to GFP destabilized by ubiquitin conjugation has been reported to inhibit degradation (11). We show here that this capacity of the GAR is also observed in yeast using a GFP substrate with a different degradation signal, one that functions independently of ubiquitin conjugation. More importantly, a GAR in the context of GFP, as in ODC, does not impair the initiation of degradation, but instead halts the process.

DISCUSSION

GAr tracts are native to the EBNA1 protein of EBV. Strain-dependent in length, they reside in the N-terminal part of the protein and function as *cis*-acting inhibitors of proteasome degradation. A GAR region has been fused to various proteasome substrates, namely p53 (10), I κ B (9), and destabilized GFP (11), and in each case inhibited their degradation. These proteins, like most substrates of the proteasome, require ubiquitin conjugation for proteasome recognition. In this paper, we document an inhibitory effect of embedding a GAR in ODC, a proteasome substrate that is degraded without ubiquitin modification (14–16). Using ODC::GAR, we have shown that a GAR can exert its effect independently of the ubiquitin system of modification and recognition. More broadly, because a GAR was found to function in a biochemical degradation reaction containing only proteasomes, ODC, and the ODC-interacting protein AZ1 as the macromolecular components, no other proteins need to be postulated to explain the action of a GAR. This does not exclude the possibility that a GAR may have additional or augmented functions that depend upon interactions with other proteins.

The question of whether a GAR modulates the initial interaction of substrate and proteasome has not been fully resolved previously (9, 10). We show here that, in the context of ODC, insertion of a GAR does not impair association and even allows the initiation of proteolysis. *In vitro* competition experiments showed that addition of a GAR insert within ODC does not diminish and may augment its proteasome interaction. *In vitro* reaction conditions using mammalian proteasomes result in less rapid and extensive ODC degradation than does *in vivo* processing: ODC in association with AZ1 has an *in vitro* half-life of 1–2 h, but an *in vivo* half-life of minutes. It is, therefore, not surprising that *in vitro* reactions failed to demonstrate

partial proteolysis of ODC::GAR. In yeast, mammalian ODC has a half-life of about 10 min. Upon expression in yeast, ODC::GAR was found to undergo partial C-terminal processing. Partial processing may require cellular components that are missing in the reaction containing purified components. Inserting a GAR did not markedly alter the rate of initiating ODC processing in yeast, but it strongly affected the outcome: complete proteolysis for ODC, and C-terminal truncation of 20, 30, or 45 amino acids in ODC::GAR. Despite a perturbed milieu of proteasome action, *rpn4 Δ* cells, like wild-type cells, processed ODC and ODC::GAR at similar rates, strengthening the inference that a GAR exerts its effect at a stage that follows initiation of proteolysis.

If a GAR can promote partial processing, why has this not been noted previously? One trivial possibility is that partial products of degradation can elude detection if they are close in size to the intact substrate or are very small. High resolution low percent acrylamide gels facilitated the analysis of the products of ODC::GAR processing. Additionally, the outcome, complete *versus* partial *versus* no proteolysis, may depend upon additional characteristics of the protein carrying a GAR: the domain structure adjacent to the GAR (31), its placement in the host protein, or whether substrate degradation is processive (32) and unidirectional (33).

ODC structure (aside from its C-terminal degradation domain) is not required for the partial processing conferred by the 30-residue GAR used in our experiments. GFP is destabilized in yeast by the addition of the 37 amino acid C-terminal degradation domain of ODC (20). Inserting the same GAR module used to create ODC::GAR between GFP and the degradation domain had similar effects as in ODC: complete degradation was converted to partial proteolysis, and the rate at which processing initiated did not significantly change. It is not clear what contiguous structures are needed for a GAR to confer partial degradation or inhibition of degradation. The GAR module failed to impair ODC degradation or impose partial degradation when inserted in two positions of ODC other than residue 424, and alternative inserts into or near position 424 did not alter degradation (Ref. 34 and results not shown). GFP consists primarily of a tightly folded β -barrel (35), and ODC to the N-terminal side of residue 424 consists of a highly structured β -sheet domain (36). It is worth exploring whether the integrity of contiguous structural domains is required to limit proteolysis, as is the case for nuclear factor- κ B processing (31).

The present findings imply that a GAR does not interfere with the initial interaction between substrate and proteasome; instead, it impedes a later step. An adequate mechanistic model of GAR inhibition must explain how, under some conditions, it allows degradation to initiate but not go to completion. Only a few cases of partial processing by the proteasome have been described previously. The proteasome carries out incomplete proteolysis to produce the transcription factors nuclear factor- κ B (37), Spt23p, and Mga2p (38) from larger precursor proteins. There is compelling evidence that the proteasome performs endoproteolytic cleavage to produce these proteins, a process that requires insertion of a polypeptide loop into the narrow proteasome insertion port (39). Furthermore, the 20S proteasome has the capacity to cleave unstructured proteins in this way (40). As all known cases of partial cleavage by the proteasome seem to involve loop insertion and endoproteolytic cleavage, it is tempting to invoke that process in the present case. However, in the known physiologic cases, loop cleavage becomes compulsory because no free end is accessible for proteasome entry. The polypeptide end that is subject to cleavage is either membrane-anchored or associated with the ribosome (39). There is no reason to believe the C terminus of ODC is

inaccessible or that the presence of a GAR, which likely assumes a random coil configuration (41), should make it so. Additionally, in yeast, the initial rate of processing either ODC or destabilized GFP is not changed by introducing the GAR. The simplest explanation of this is that proteasome interaction and initial cleavage is not altered by the GAR, but that the process halts in one case and not the other. ODC insertion begins at the C terminus.² In ODC::GAR, processing begins as for ODC, but then fails.

The GAR-induced halt to degradation could result from one of several mechanisms. Eukaryotic proteasomes contain three distinct types of proteolytic sites, which cleave preferentially after large hydrophobic, basic, or acidic residues (42). One may speculate that, after encountering the poorly digestible GAR at or near its proteolytic sites, the proteasome responds with some form of allosteric regulation (43) that pauses substrate insertion. Alternatively, the GAR may in some more direct manner impede access to distal hydrophobic, basic, or acidic residues within the substrate protein. However, proteasomes produce peptides of peak sizes 2–3, 9–10, and 20–30 residues (44); it is hard to imagine how a mechanism based on restricted digestion could explain the effect of a GAR as short as seven residues. We prefer a model whereby the GAR impairs ATP-driven insertion of substrate. Concerted hydrolysis of ATP by the six distinct ATPase proteins of the 19S proteasome regulatory complex is, by analogy with structurally related bacterial proteases (45, 46), likely coupled to motions of components that move substrates forward. One attractive possibility is that power strokes (47) within the 19S complex move the substrate, and that a GAR sequence of sufficient length eludes their reach. The small, uncharged amino acids of a GAR sequence could fail to provide traction between the peptide and the power stroke loops of the AAA motor. The reach of the power stroke can be approximated by the dependence of inhibitory effectiveness on GAR length. A 30-residue GAR presents an insurmountable barrier, whereas a GAR of 7 residues is inhibitory almost half the time. The length of an extended 7-residue polypeptide chain correlates well with the estimated power stroke length of about 20 Å in other AAA motors,³ such as bacteriophage T7 helicase (48). Insertion stalls when the reach of the proteasome exceeds its grasp.

Acknowledgment—We thank George Oster, University of California, Berkeley, for stimulating discussions of ATP-dependent molecular motors.

REFERENCES

- Tortorella, D., Gewurz, B. E., Furman, M. H., Schust, D. J., and Ploegh, H. L. (2000) *Annu. Rev. Immunol.* **18**, 861–926
- Hewitt, E. W. (2003) *Immunology* **110**, 163–169
- Leight, E. R., and Sugden, B. (2000) *Rev. Med. Virol.* **10**, 83–100
- Falk, K., Gratama, J. W., Rowe, M., Zou, J. Z., Khanim, F., Young, L. S., Oosterveer, M. A., and Ernberg, I. (1995) *J. Gen. Virol.* **76**, Pt 4, 779–790
- Levitskaya, J., Coram, M., Levitsky, V., Imreh, S., Steigerwald-Mullen, P. M., Klein, G., Kurilla, M. G., and Masucci, M. G. (1995) *Nature* **375**, 685–688
- Levitskaya, J., Sharipo, A., Leonchiks, A., Ciechanover, A., and Masucci, M. G. (1997) *Proc. Natl. Acad. Sci. U. S. A.* **94**, 12616–12621
- Yin, Y., Manoury, B., and Fahraeus, R. (2003) *Science* **301**, 1371–1374
- Voges, D., Zwirckl, P., and Baumeister, W. (1999) *Annu. Rev. Biochem.* **68**, 1015–1068
- Sharipo, A., Imreh, M., Leonchiks, A., Imreh, S., and Masucci, M. G. (1998) *Nat. Med.* **4**, 939–944
- Heessen, S., Leonchiks, A., Issaeva, N., Sharipo, A., Selivanova, G., Masucci, M. G., and Dantuma, N. P. (2002) *Proc. Natl. Acad. Sci. U. S. A.* **99**, 1532–1537
- Dantuma, N. P., Heessen, S., Lindsten, K., Jellne, M., and Masucci, M. G. (2000) *Proc. Natl. Acad. Sci. U. S. A.* **97**, 8381–8385
- Glickman, M. H., and Ciechanover, A. (2002) *Physiol. Rev.* **82**, 373–428
- Tellam, J., Sherritt, M., Thomson, S., Tellam, R., Moss, D. J., Burrows, S. R., Wiertz, E., and Khanna, R. (2001) *J. Biol. Chem.* **276**, 33353–33360
- Murakami, Y., Matsufuji, S., Kameji, T., Hayashi, S., Igarashi, K., Tamura, T., Tanaka, K., and Ichihara, A. (1992) *Nature* **360**, 597–599
- Zhang, M., Pickart, C. M., and Coffino, P. (2003) *EMBO J.* **22**, 1488–1496
- Coffino, P. (2001) *Nat. Rev. Mol. Cell Biol.* **2**, 188–194
- Sambrook, J., and Russell, D. W. (2001) *Molecular Cloning: A Laboratory Manual*, 3rd Ed., Cold Spring Harbor Laboratory Press, Cold Spring Harbor, NY
- Laux, G., Perriacaudet, M., and Farrell, P. J. (1988) *EMBO J.* **7**, 769–774
- Baer, R., Bankier, A. T., Biggin, M. D., Deininger, P. L., Farrell, P. J., Gibson, T. J., Hatfull, G., Hudson, G. S., Satchwell, S. C., Seguin, C., Tuffnell, P. S., and Barrell, B. G. (1984) *Nature* **310**, 207–211
- Hoyt, M. A., Zhang, M., and Coffino, P. (2003) *J. Biol. Chem.* **278**, 12135–12143
- Mumburg, D., Muller, R., and Funk, M. (1995) *Gene* **156**, 119–122
- Chen, P., Johnson, P., Sommer, T., Jentsch, S., and Hochstrasser, M. (1993) *Cell* **74**, 357–369
- Kisselev, A. F., and Goldberg, A. L. (2001) *Chem. Biol.* **8**, 739–758
- Almud, J. J., Oliveira, M. A., Kern, A. D., Grishin, N. V., Phillips, M. A., and Hackert, M. L. (2000) *J. Mol. Biol.* **295**, 7–16
- Dantuma, N. P., and Masucci, M. G. (2002) *FEBS Lett.* **529**, 22–26
- Toth, C., and Coffino, P. (1999) *J. Biol. Chem.* **274**, 25921–25926
- Miyazaki, Y., Matsufuji, S., Murakami, Y., and Hayashi, S. (1993) *Eur. J. Biochem.* **214**, 837–844
- Lee, D. H., and Goldberg, A. L. (1996) *J. Biol. Chem.* **271**, 27280–27284
- Fleming, J. A., Lightcap, E. S., Sadis, S., Thoroddsen, V., Bulawa, C. E., and Blackman, R. K. (2002) *Proc. Natl. Acad. Sci. U. S. A.* **99**, 1461–1466
- Li, X., Zhao, X., Fang, Y., Jiang, X., Duong, T., Fan, C., Huang, C. C., and Kain, S. R. (1998) *J. Biol. Chem.* **273**, 34970–34975
- Lee, C., Schwartz, M. P., Prakash, S., Iwakura, M., and Matouschek, A. (2001) *Mol. Cell* **7**, 627–637
- Akopian, T. N., Kisselev, A. F., and Goldberg, A. L. (1997) *J. Biol. Chem.* **272**, 1791–1798
- Navon, A., and Goldberg, A. L. (2001) *Mol. Cell* **8**, 1339–1349
- Ben-Shahar, S., Komlos, A., Nadav, E., Shaked, I., Ziv, T., Admon, A., DeMartino, G. N., and Reiss, Y. (1999) *J. Biol. Chem.* **274**, 21963–21972
- Tsien, R. Y. (1998) *Annu. Rev. Biochem.* **67**, 509–544
- Kern, A. D., Oliveira, M. A., Coffino, P., and Hackert, M. L. (1999) *Structure Fold Des.* **7**, 567–581
- Lin, L., DeMartino, G. N., and Greene, W. C. (1998) *Cell* **92**, 819–828
- Hoppe, T., Matuschewski, K., Rape, M., Schlenker, S., Ulrich, H. D., and Jentsch, S. (2000) *Cell* **102**, 577–586
- Rape, M., and Jentsch, S. (2002) *Nat. Cell Biol.* **4**, E113–E116
- Liu, C. W., Corboy, M. J., DeMartino, G. N., and Thomas, P. J. (2003) *Science* **299**, 408–411
- Leonchiks, A., Liepinsh, E., Barishev, M., Sharipo, A., Masucci, M. G., and Otting, G. (1998) *FEBS Lett.* **440**, 365–369
- Cardozo, C., Vinitzky, A., Michaud, C., and Orłowski, M. (1994) *Biochemistry* **33**, 6483–6489
- Gaczynska, M., Osmulski, P. A., Gao, Y., Post, M. J., and Simons, M. (2003) *Biochemistry* **42**, 8663–8670
- Kohler, A., Cascio, P., Leggett, D. S., Woo, K. M., Goldberg, A. L., and Finley, D. (2001) *Mol. Cell* **7**, 1143–1152
- Niwa, H., Tsuchiya, D., Makyio, H., Yoshida, M., and Morikawa, K. (2002) *Structure* **10**, 1415–1423
- Kenniston, J. A., Baker, T. A., Fernandez, J. M., and Sauer, R. T. (2003) *Cell* **114**, 511–520
- Oster, G., and Wang, H. (2003) *Trends Cell Biol.* **13**, 114–121
- Singleton, M. R., Sawaya, M. R., Ellenberger, T., and Wigley, D. B. (2000) *Cell* **101**, 589–600

² A. I. MacDonald, M. Zhang, and P. Coffino, manuscript in preparation.

³ Personal communication, George Oster, University of California, Berkeley.